

Supplementary Information

Two-Dimensional Vanadium Tetrafluoride with Antiferromagnetic Ferroelasticity and Bidirectional Negative Poisson's Ratio

Lei Zhang^{ab}, *Cheng Tang*^{ab}, *Aijun Du*^{*ab}

^a School of Chemistry and Physics, Queensland University of Technology, Gardens Point
Campus, Brisbane, QLD 4000, Australia

^b Centre for Materials Science, Queensland University of Technology, Gardens Point Campus,
Brisbane, QLD 4000, Australia

Table S1. The difference between calculated lattice constants and the experimental values for bulk VF_4 by different functionals and PBE+U methods with variant U values.

	PBE	LDA	optB88	optB86b	PBEsol	PBE+U		
						U=1	U=2	U=3
Δa	0.052	-0.079	0.041	0.063	0.022	0.067	0.101	0.095
Δb	0.005	-0.297	-0.189	-0.202	-0.187	0.010	-0.011	0.015
Δc	0.042	-0.256	-0.089	-0.075	-0.083	0.059	0.068	0.074

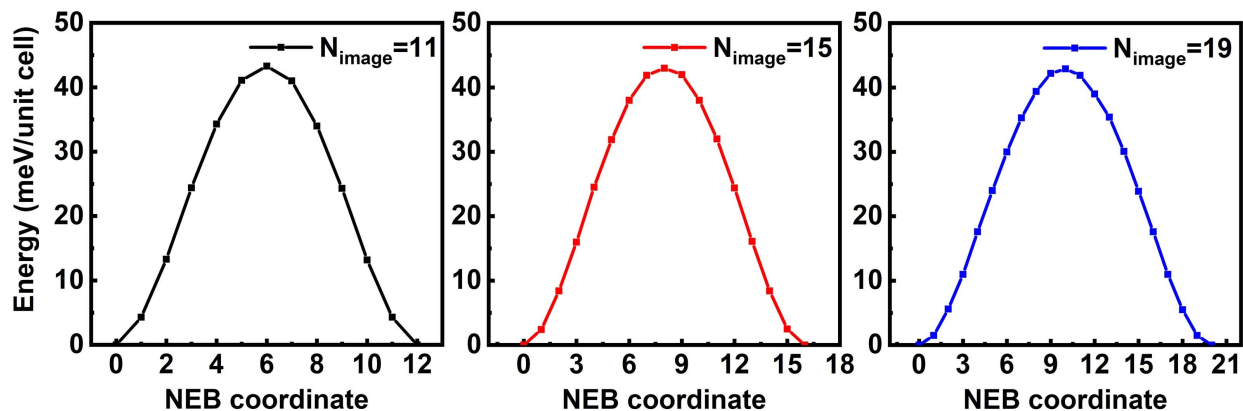


Figure S1. The NEB results calculated using 11, 15, and 19 images for the ferroelastic transition of VF_4 monolayer. The transition barriers calculated using 11, 15, and 19 images are 43.3 meV/unit cell, 43.0 meV/unit cell, and 42.9 meV/unit cell, respectively. Hence, the transition barrier can converge to 1 meV/unit cell even with a low number of image of 11.

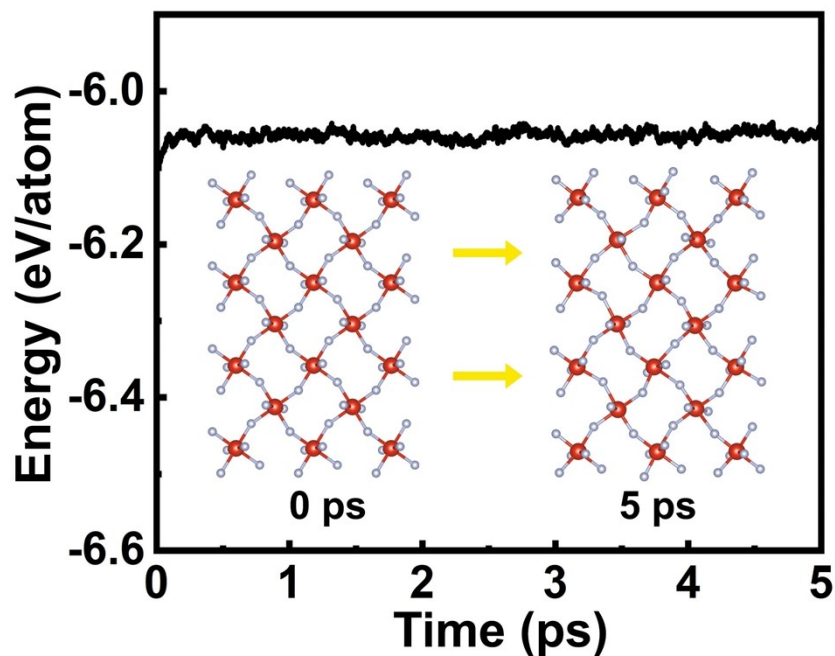


Figure S2. The energy evolution of VF_4 monolayer during AIMD of 5 ps at 300 K. The insets are the initial and final atomic structure.

Table S2. Total energy of VF_4 monolayer in different magnetic configurations. The energy of AFM-2 configuration is set to 0 for comparison. The energy of non-magnetic state is 1.54 eV/unit cell higher than the AFM-2 state, suggesting the robust magnetism in 2D VF_4 .

Configuration	FM	AFM-1	AFM-2	AFM-3
ΔE (meV)	46.89	23.90	0	23.35

Table S3. The MAE (μeV per V atom) with respect to the easy-axis direction.

Direction	[100]	[010]	[110]	[101]	[011]	[111]	[001]
MAE	0	28.92	26.81	39.77	34.23	13.24	35.84

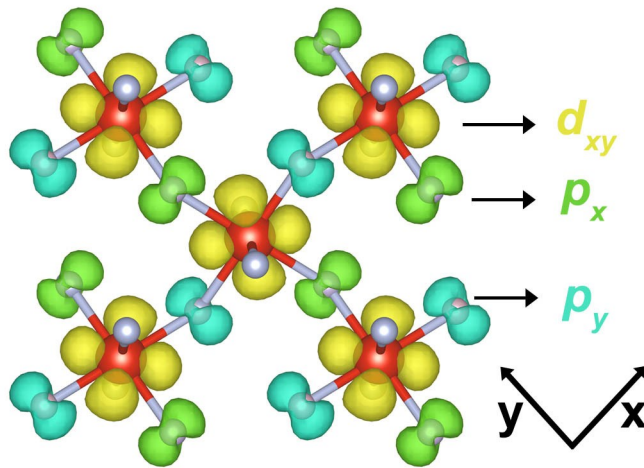


Figure S3. The real-space squared wave-function corresponding to the highest valence band at Gamma point. The global coordination axis is rotated to align the VF_6 octahedra. The d_{xy} orbitals of V atoms and $p_{x/y}$ orbitals of F atoms are vividly shown.

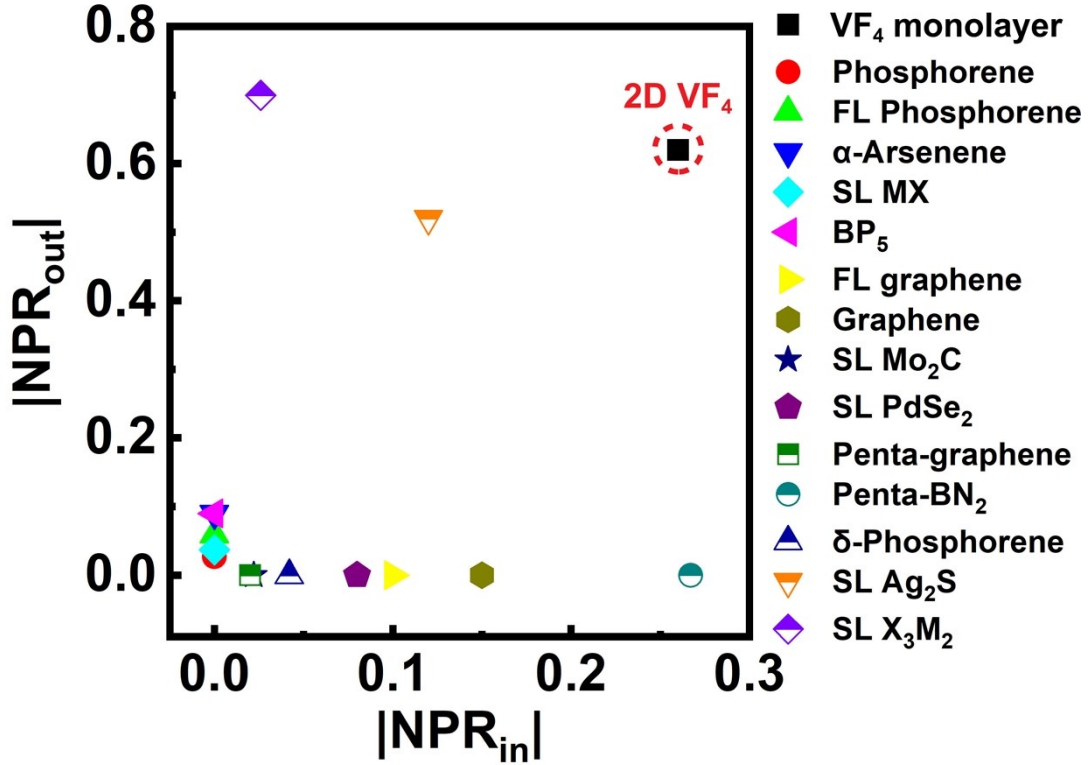


Figure S4. The in-plane and out-of-plane NPRs for 2D VF_4 , phosphorene,¹ few-layer (FL) phosphorene,² α -arsenene,³ single-layer (SL) MX (M = Ge, Sn; X = S, Se),⁴ BP_5 ,⁵ FL graphene,⁶ graphene,⁷ SL Mo_2C ,⁸ SL $PdSe_2$,⁹ penta-graphene,¹⁰ penta- BN_2 ,¹¹ δ -phosphorene,¹² SL Ag_2S ,¹³ and SL X_3M_2 .¹⁴ For clarity, we plot the absolute values here and if it does not exist, we set it to 0. It can be seen that 2D VF_4 possess balanced bidirectional auxeticity and the values of NPR along both directions are among the highest values reported so far.

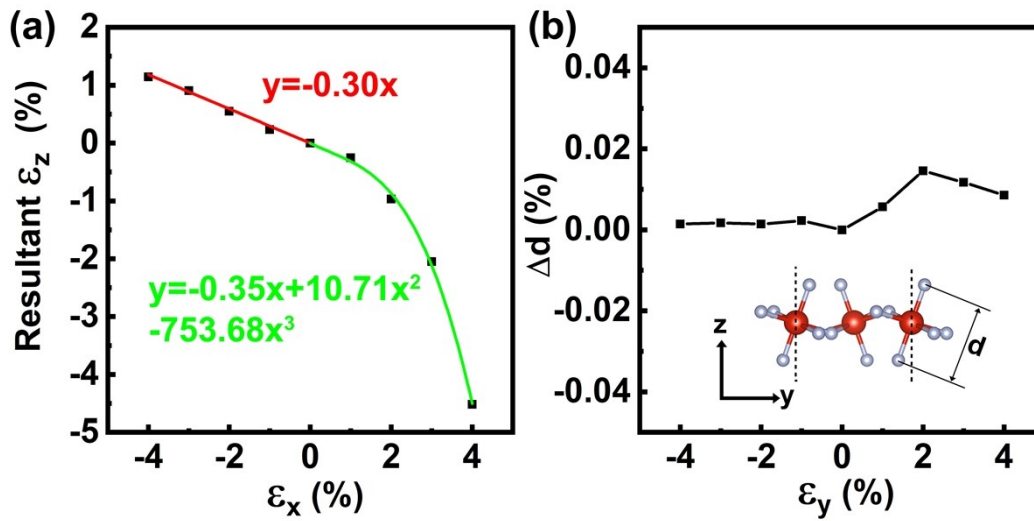


Figure S5. (a) Resultant out-of-plane strain as a function of applied strain along the x-direction. The v_{out} is obtained by fitting $\varepsilon_{rs} = -a\varepsilon_s + b\varepsilon_s^2 + c\varepsilon_s^3$,¹³ where ε_s and ε_{rs} represent the applied and resultant strain respectively, and then a can be regarded as v_{out} . The calculated v_{out} is 0.30 and 0.35 for compressional and tensile strain applied along the x-direction, respectively. (b) The variation of the distance between the upper and lower F atoms in a VF_6 octahedron upon strain along the y-direction. Clearly, the variation is quite small (less than 0.02%).

References

1. Y. Du, J. Maassen, W. Wu, Z. Luo, X. Xu and P. D. Ye, *Nano Lett.*, 2016, **16**, 6701-6708.
2. J.-W. Jiang and H. S. Park, *Nat. Commun.*, 2014, **5**, 4727.
3. J. Han, J. Xie, Z. Zhang, D. Yang, M. Si and D. Xue, *Appl. Phys. Express*, 2015, **8**, 041801.
4. X. Kong, J. Deng, L. Li, Y. Liu, X. Ding, J. Sun and J. Z. Liu, *Phys. Rev. B*, 2018, **98**, 184104.
5. H. Wang, X. Li, J. Sun, Z. Liu and J. Yang, *2D Mater.*, 2017, **4**, 045020.
6. S. Woo, H. C. Park and Y.-W. Son, *Phys. Rev. B*, 2016, **93**, 075420.
7. K. V. Zakharchenko, M. I. Katsnelson and A. Fasolino, *Phys. Rev. Lett.*, 2009, **102**, 046808.
8. B. Mortazavi, M. Shahrokhi, M. Makaremi and T. Rabczuk, *Nanotechnology*, 2017, **28**, 115705.
9. G. Liu, Q. Zeng, P. Zhu, R. Quhe and P. Lu, *Comput. Mater. Sci.*, 2019, **160**, 309-314.
10. S. Zhang, J. Zhou, Q. Wang, X. Chen, Y. Kawazoe and P. Jena, *Proc. Natl. Acad. Sci. U.S.A.*, 2015, **112**, 2372-2377.
11. M. Yagmurcukardes, H. Sahin, J. Kang, E. Torun, F. M. Peeters and R. T. Senger, *J. Appl. Phys.*, 2015, **118**, 104303.
12. H. Wang, X. Li, P. Li and J. Yang, *Nanoscale*, 2017, **9**, 850-855.
13. R. Peng, Y. Ma, Z. He, B. Huang, L. Kou and Y. Dai, *Nano Lett.*, 2019, **19**, 1227-1233.
14. Y. Chen, X. Liao, X. Shi, H. Xiao, Y. Liu and X. Chen, *Phys. Chem. Chem. Phys.*, 2019, **21**, 5916-5924.